Strojniški vestnik - Journal of Mechanical Engineering vol(yyyy)no, p-p
DOI code
Original Scientific Paper
Received for review: yyyy-mm-dd
Received revised form: yyyy-mm-dd
Accepted for publication: yyyy-mm-dd

Selected microstructural and mechanical properties of open-cell metal foams

Wojciech Depczyński*
Kielce University of Technology, Faculty of Mechatronics and Mechanical Engineering

The microstructural and mechanical properties of open-cell metal foams have been investigated in numerous studies. Due to materials used and manufacturing technologies, presented foam has specific, unique properties among foams produced by other methods. The aim of the article is to study the microstructural and mechanical properties of metal foams manufactured by the reduction of metal oxides during sintering. The experiment was carried out for four sets of sintered powders: ASC 100.29, ASC 100.29 + C, DISTALOY SE, DISTALOY SE + C. An important element of research was to measure the absorption of kinetic energy, using a device that measures the material's dissipated kinetic energy. The research revealed that modifying the microstructural and mechanical properties of open-cell Fe-based foams, could lead to wider application as a light-weight structural or energy absorbing materials, filters, heat exchange surfaces areas, etc.

Keywords: open-cell metal foams, Fe-based foams, reduction of metal oxides, space holder technique, energy dissipation.

Highlights*:*

- Fe-based metal foams were produced by low-cost sintering processes
- Reduction of Fe (III) oxide space holder and Cu application caused creation of homogenous structure with open porosity
- Average pore diameter has not exceeded 100 μm and porosity level were 67.9% and 80.3% depending on the iron powder composition.
- Speed and acceleration of the beater at the moment of impact was determined using a time-lapse camera
- Fe-based foams find application as light-weight structural materials, or dissipative and energy-absorbing materials, or filters, catalyst substrates and heat exchange surface areas.

0 INTRODUCTION

Iron has been used as the basic material for the production of everyday use tools or weapons since prehistoric times. The 19th century saw the emergence of new technologies for iron alloys manufacture, with the most important – steel technology, the products of which are commonly used in construction materials nowadays. Dynamic expansion of the new technologies created a need for new class materials characterized by unique properties.

Looking for the inspiration, engineers and scientist all over the world used ideas obtained from the best source of knowledge – wild nature. Ashby said [1]: "When modern man builds large load-bearing structures, he uses dense solids: steel, concrete, glass. When Nature does the same, she generally uses cellular materials: wood, bone, coral" [2,3].

Experiments were carried out to verify various manufacturing techniques and applications of structural materials with a porous structure. One of the very first successful studies on porous materials led to the creation of a porous polymer structure, for polymer membrane structure [2] and polymer porous electrolytes[3]. This was just the beginning. Research on metal based porous materials became much more intensive [4]. Several production methods were invented to produce metal foams with closed or open porosity and pore sizes from a micrometer to several millimetres of crystal or amorphous structures [5,6].

This effort contributed to the development of various applications for porous structures: aluminium sound absorbers copper heat exchangers or nickel battery electrodes. Arwade [7] wrote: "Steel is one of the most widely used engineering materials, yet today no foam using steel as the base material is commercially

*Corr. Author's Address: Kielce University of Technology, Faculty of Mechatronics and Mechanical Engineering, 25-314 Kielce, Al. Tysiąclecia PP 7, Poland, wdep@tu.kielce.pl

available". Therefore, there is a great need to further research into the manufacturing techniques and properties of Fe-based porous materials [8,9].

The motivation to carry out the research was a fact that previously known studies in the field of open-cell metal foams do not describe adequately Fe-foam properties for energy absorption applications. The aim of the study was to investigate structure and selected dynamic parameters – energy dissipation in order to determine the scope of the Fe-foam.

One of the most efficient methods of manufacturing iron based porous materials is sintering, for its low cost. There is no need for achieving iron melting temperature to obtain the desired structure. Porosity is provided by the application of a space holder or foaming agent. Bekoz [10] investigated sintered low alloy steel foams produced using the space holder-water leaching technique and obtained the product with porosity ranging from 47.8 to 70.9%, depending on the space holder size (500 – 1200 μm). Murakami [11] studied methods for manufacturing iron foams using CO and CO_2 as foaming gases. The final product had the maximum porosity of 55% and average pore size of 500 μm. Each of these methods used compression during the process of sample preparation, which affected the end result.
The sintered porous iron based material discussed in this article differs from the conventionally produced iron foams in that no compression treatment of base powders is applied [12].

1 MATERIALS AND PROCESSING

The authors of this article propose a method of producing porous foams by sintering metal powders. The method uses Fe (III) oxide both as the foaming agent and as the space holder. By reacting with the atmosphere used during sintering, Fe (III) oxide is reduced to form hollow space inside. Another important factor, which strongly influences the structure of the sintered material, is the presence of H_2O vapors, CO and, optionally, CO_2. These gases act as the foaming agent, which being released from the space occupied by the sinter creates open connections between the pores. The method was patented by the author [13]. This technology of forming porous materials has already been used for the preparation of porous layers of copper (Cu + CuO and Cu_2O sintered in the reducing atmosphere of dissociated ammonia) applicable as coatings for heat exchangers working under the nucleate boiling mode [14,15]. The resultant porosity was 45-70% for the coating thickness of 0.2 to 1 mm. The open pores were about 50 - 100 μm in size. Good results achieved in the production of porous copper layers inspired further efforts in an attempt to use Fe and its oxides.

2 EXPERIMENTAL

Metallic precursor composition was designed based on four sets of atomized iron base powders: ASC 100.29, ASC 100.29 + C, DISTALOY SE, DISTALOY SE + C. All of them were mixed with copper - diffusion catalyst and iron (III) oxide as the foaming agent and space holder. Every single ingredient of the sintered composition was in the form of powder. Prepared specimens were not compacted at any internal ways, only with external gravity reactions. The shape of dies (steel containers) determined dimensions of the sintered samples. The containers size was 30 mm/ 50 mm/100 mm. The chemical composition of the iron-based powders under investigation is shown in Table 1.

Table 1. *Chemical composition of iron-based powders*

Powder	Chemical composition, %					
	C	Cu	Ni	Mo	O	Fe
ASC 100.29	< 0.01	-	-	-	-	bal
DISTALOY SE	< 0.01	1.5	4	0.5	-	bal

To have a closer look at the particles dimensions and shape of all applied powders, scanning electron microscopy (JSM-7100F) was applied. Figures 1a, 1b, 1,c, 1d shows the SEM results of all applied powders.
Table 2 presents content of applied powders. To simplify the designation of the prepared sets, the specimens were marked as: ASC for ASC 100.29 base powder composition and SE for DISTALOY SE base powder composition.

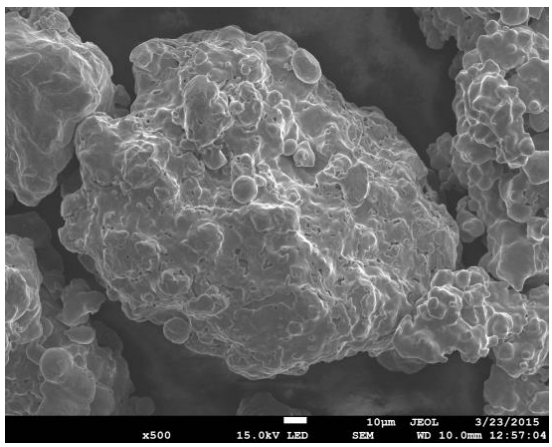

Fig. 1a. *SEM images of applied ASC 100.29 powder*

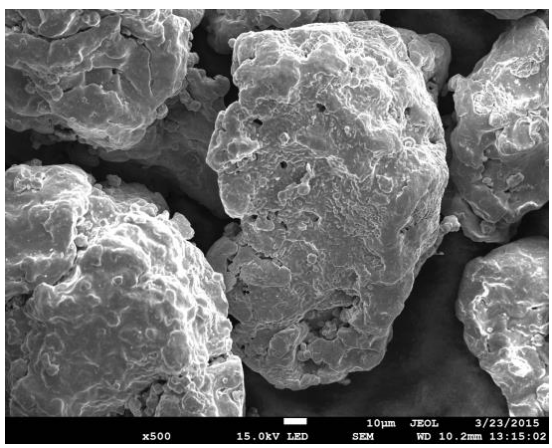

Fig. 1b. *SEM images of applied DISTALOY SE powder*

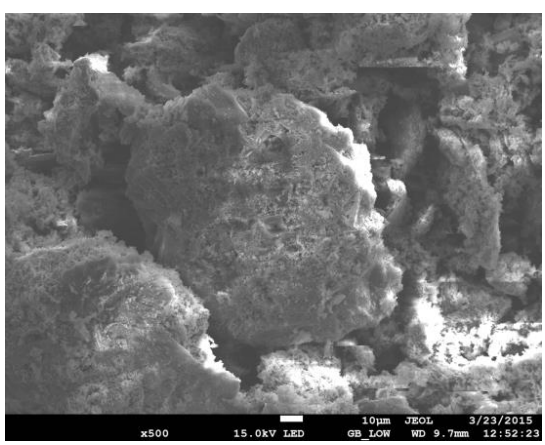

Fig. 1c. *SEM images of applied iron (III) oxide powder*

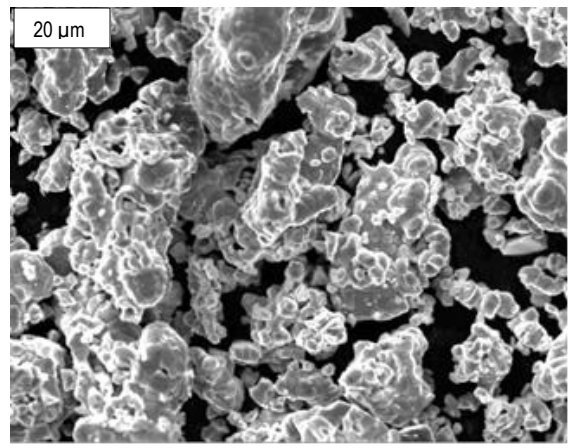

Fig. 1d. *SEM images of applied copper powder*

Table 2. *Total content of applied materials, as a percentage*

Powders	Composition [%]			
	ASC	ASC+C	SE	SE+C
ASC 100.29	85	85	-	-
DISTALOY SE	-	-	85	85
Cu	5	5	5	5
Iron (III) oxide	10	10	10	10
C	-	0,8	-	0,8

The specimens were sintered at a temperature of 1130^{O}C in a tube furnace. The oxides reducer gas – hydrogen - was obtained in the process of ammonia dissociation.

After sintering for 50 minutes, the specimens were moved to the cooling chamber for crystallization. High temperature and hydrogen affected the iron (III) oxide reduction. Hollow spaces appeared inside the solid structure. The iron (III) oxide reduction was the major factor in porosity formation. The edges of iron based powder particles adhered to one another thus creating diffusion bridges. At 1085^{O}C, the copper powder underwent a phase transition from the solid to the liquid phase. The melted copper acted as the reaction catalyst.

3 RESULTS

3.1 Microstructural characterisation

The samples were sintered with a steel container to form an absorbent element. Kujime [16] chosen spark erosion as the best technology of machining porous carbon steel, therefore

method has been applied in this research. Samples for observing the microstructure were prepared by cutting out larger elements using the method recommended by Kujime.The process of spark erosion was used to obtain 14 mm high and ϕ16 mm in diameter specimens with symmetric geometry. Metallographic samples were prepared. Cylindrical shape samples were cut along their cross sections. Some of them were etched using ethyl alcohol for optical microscope analysis. The microstructure of the porous material obtained was evaluated using SEM images featuring individual grains in the material. Copper in the liquid state surrounded the globular iron powder particles. The copper melted iron grain boundaries and created the grain to grain "diffusion bridge". The results can be seen in Figures 2a and 2b, 2c.

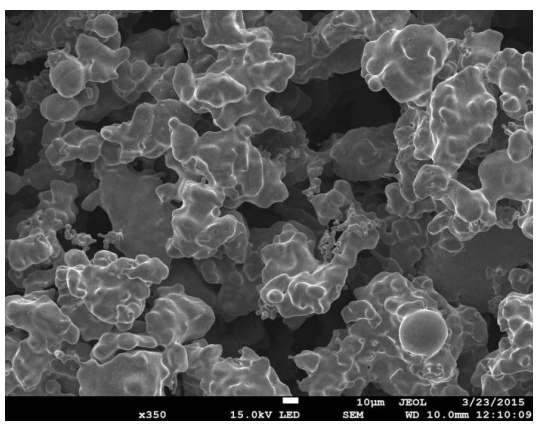

Fig. 2a. *SEM images of sintered iron base ASC specimens*

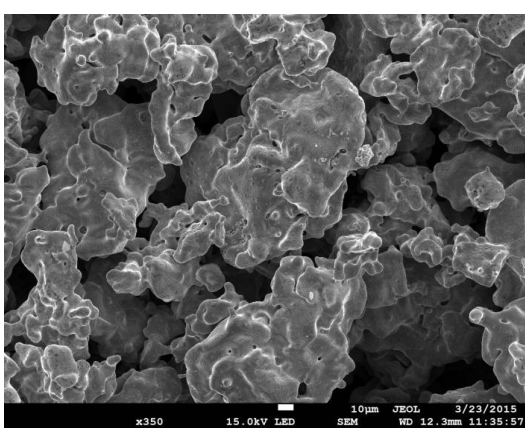

Fig. 2b. *SEM images of sintered iron base SE specimens*

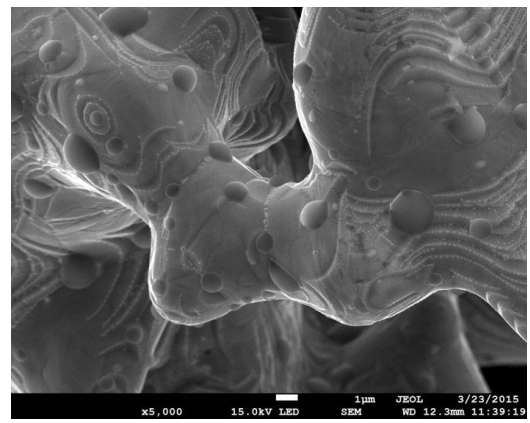

Fig. 2c. *SEM images of sintered iron base SE specimens (grains diffusion bridge)*

The sintering process generated open porosity in the structure. Estimation of average pore size was not easy because of the random arrangement of pores. The pore diameter was approximately 100 μm. It was was measured on metallographic lateral deflection using NIS 4.20 image analysis software and equivalent diameter was determined on cross-section. According to the Cavalieri-Hecquert principle, it can be assumed that this is a representative measurement. The reduction of Fe_2O_3 space holder had produced an interconnected network of open pores. Figure 2(c) shows the grain diffusion bridge.

The porosity level was assessed using optical microscopy. ASC 100.29 and DISTALOY SE (DIST SE) with porosity from 67.9 % (SE 1) to 77.8 % (SE 2) for ASC base powder and 75.7 % to 80.3 % for DISTALOY SE were used. Porosity was determined over the cross section of the sample by means of NIKON NIS 4.12 image analysis software. Cavalieri-Hacquert principle was applied.

3.2 Dynamical testing

An important element of studying the mechanical properties of metallic porous materials is to measure the absorption of kinetic energy. The measurement was made using a device - specially designed to carry out experiments - that measures the material's ability to dissipate kinetic energy (see Fig. 3).

The attempt consisted in striking successively (six) cuboids filled with foam, using a ram of

known mass. The speed and acceleration of the beater at the moment of impact was determined using a time-lapse camera (see Fig. 4).

Fig. 3. *The device for measure kinetic energy absorption*

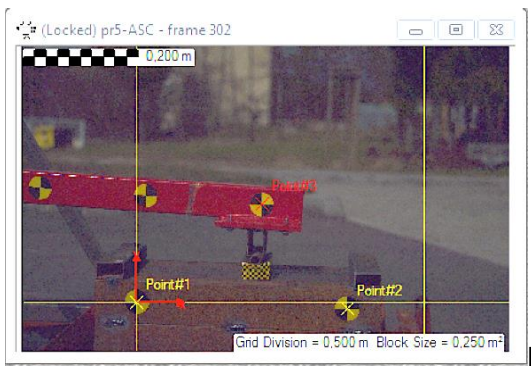

Fig. 4. *The moment of ram impact – frame by TEMA Motion*

The TEMA Motion application was used to measure the speed and acceleration of a moving ram.

Four containers (presented in Figure 5) comprise compositions of the sintered powders: ASC, ASC + C, SE, SE + C. The fifth container was filled with sawdust, and the sixth was a hollow.

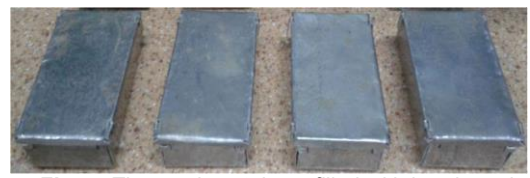

Fig. 5. *The steel containers filled with iron-based porous materials compositions.*

Due to design of the measuring device, the test parameters for each of the six tests were approximately constant. The hammer weight was m = 2.3 [kg]. The maximum deceleration is shown in graphs obtained by TEMA Motion, which are presented in Figure 6.

Graphs were received from measurements of a sample made of all powder mixtures.

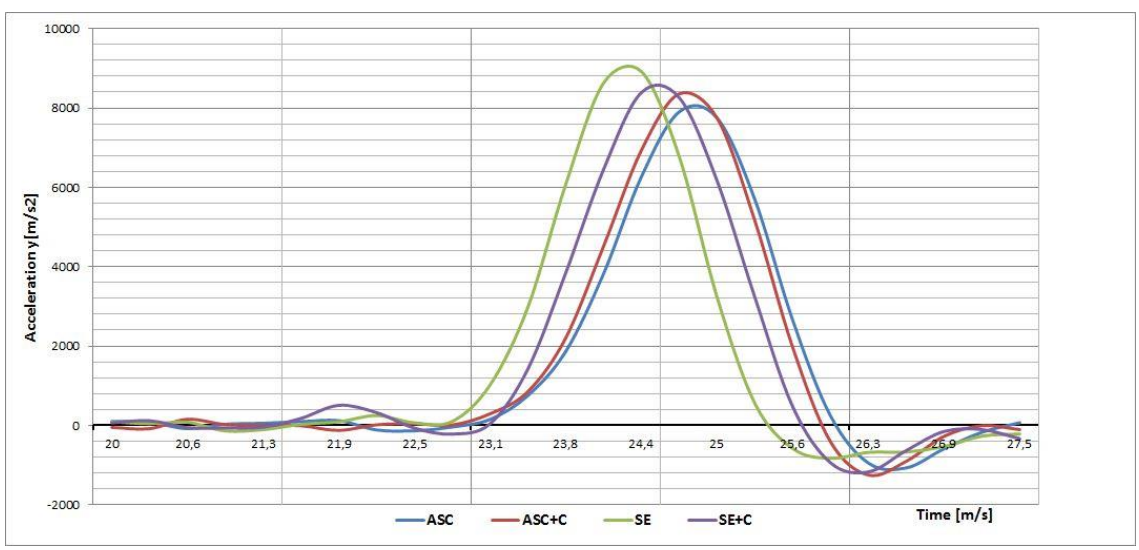

Fig. 6. *Graph of deceleration in time for ASC, ASC + C, DISTALLOY SE and DISTALLOY SE + C samples.*

The analysis of above graphs allows to determine the acceleration value at 8000 [m/s^2], that is, approximately 800 G. The speed at the moment of impact was 11 [m/s]. The impact occurred in 25.5 milliseconds, and then the hammer bounced off the tested material. The kinetic energy of impact was 139,15 J.
The degree of deformation of tested absorbers is shown in Figure 7 and cross-section in Figure 8.

Fig. 7. *Deformed steel containers of tested absorbers including calibration (sawdust and empty one – last two containers).*

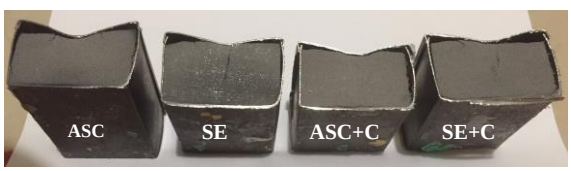

Fig. 8. *Cross section of the deformed steel containers of tested absorbers.*

Starting on the right side turn: the empty container (used for calibration) was completely destroyed. The container covered with sawdust - also was completely destroyed. The container filled with ASC, ASC + C, SE, SE-C blends also were deformed but to varying degrees. They absorbed a certain amount of kinetic energy of the impact depending on the filling properties.
At the moment of impact (in 25.5 millisecond), the ram came into contact with test sample. The contact lasted up to 37 milliseconds. This caused a deformation of 0.013 [m]. In an analogous manner is possible to determine the deformation in remaining samples: ASC-C, SE, SE + C. The measured values are presented in Table 3.

Table 3. *Deformation of steel containers filling of porous materials*

Absorber's material	Deformation [m]	Mass [g]
ASC	0,013	443,20
ASC + C	0,008	435,32
SE	0,007	450,84
SE + C	0,009	430,10

4 DISCUSSION

The high porosity level in all four materials under investigation was caused by the coexistence of optimal conditions: heating rate, heating temperature and composition of the precursor powder. Sintering at 1130^{0}C for 50 minutes resulted in the uniform temperature distribution. The rapid heating rate and lower heating temperature could be the possible causes of iron (III) oxide reduction failure and prevention of pore formation. Iron did not transfer into the eutectic phase, however, iron grain edges melted. Copper powder changed into the liquid phase and increased energy on the iron grains boundaries. Copper was also used as the interconnecting factor. Figure 2c presents a globular shape of iron powder grain surrounded by liquid copper creating the "diffusion bridge".

Research on iron based porous material by Murakami, Ohara et al. [11] contributed to better understanding of the nature of iron foam processing in the semi-liquid phase. Using hematite [Fe_2O_3] as the foaming agent, the authors succeeded in producing a material with maximum 55% porosity in the structure 1% hematite content and an average pore size of 500 to 800 µm. When the quantity of hematite exceeded 1%, the porosity level decreased. As they said, "While the increase in the hematite content increases the amount of foaming gas and consequently the porosity, the excess amount of gas generated by the addition of an excess amount of the foaming agent appears to decrease the porosity"[…]" However, the addition of an excess amount of hematite may yield pores with a high pressure in the melt, which may bubble out from the melt". What is interesting, when hematite was relatively high, 2%, pore diameters decreased with an increase in porosity level. This corresponds to the results obtained in this study; an application of 10% Fe (III) oxide led to the iron foam characterized by pore diameters of approximately 100 µm.

The formation of macro and micro porosity was observed by Bekoz [10], during research on low alloy steel foams. As a result of applying carbamide as the space holder, specimens with macro pores with exceeding 1000 µm in diameter were produced. What is

interesting, sintering the Distaloy AB steel powder as the base material at 1200^{O} C for 60 minutes contributed to the formation of micropore diameter of less than 100 μm. The sintering conditions were very similar to those discussed in this article. It is, however, possible that micro porosity obtained by Bekoz *et al.* was the side effect of the study of carbamide space holder.

It is very important to discuss different ways of porosity formation in metallic materials. A direct stream of external gases applied to the melted material was the foaming agent adopted by Kujime [15]. This method allowed fabricating a material with a uniform pore size and distribution. Kujime *et al.* studied porous carbon steel manufactured by the continuous zone melting method in a pressurized mixture of hydrogen and helium gases. The resultant structure had the porosity of 26 – 44% and average pore diameters between 500 and 700 μm. As can be seen, their research resulted in producing the structure characterized by higher pore diameters and lower porosity levels compared to the structure described in this paper. The gas blowing method differed from the common ways of porosity formation such as powder metallurgy and there was a need to describe this process. Kujime's conclusion was the following, "The porosity of lotus steel increases with the increasing partial pressure of hydrogen gas".

Another important factor that defines a porous structure is the gas pressure exerted on the material during the sintering processes. All specimens studied in this paper were prepared under the pressure of 1 bar. The influence of air overpressure on the porosity level has been investigated by Saadatfar [17], who characterized the metallic foams using X-ray micro-CT. Their study was devoted to metal foams created using forming agents different from iron compositions. Therefore there is a need for preparing similar research for iron-based materials, however the author himself investigated the micro-CT research of presented foam [18].

Metallographic microscopy was very useful for describing percentage porosity level and pores diameter estimation. Unfortunately it was not accurate enough to define internal structure the grains diffusion. SEM imagining was successfully applied to solve this issue. Maire [19] in his structural characterization of solid foams said, "The complex 3D architecture of solid foams requires observation techniques permitting a high depth of field. Amongst the standard available techniques, only SEM shows enough depth of focus to apprehend the structure of these materials". Successively the author applied 3D imagining modeling of metallic porous materials containing diffusion bridges produced by the sintering of metal [20]

Uniformity of porous structure has been caused by occurrence of favourable factors; mechanical powder mixing and oxides reduction at steady temperature. Research carried out by A. Rabei [21] contributed to creating iron based porous structure, where the pre-sintering vibration process caused differences between porosity on the spheres walls and the matrix - iron powder particles has coated globular shaped hollow spheres on the walls during the vibrations, where rest of the iron powder was not compressed or attached to any external element.

Metal foams are used, among others in shock absorbing elements and energy absorbing bullets and shardsIn recent years, there have been appeared publications addresing this thematic area. Publications include both experimental and FEM research method analysis [22,23,24].

Energy absorption by tested elements show, that sample ASC is most effective, while biggest decelaraction has SE sample. ASC+C and SE +C samples were similarly preserved – both showed similar deceleration. Deformation of the samples corresponds to the deceleration: ASC has greater deformation and SE smaller. Also SE sample has reduced porosity, due to the largest sample mass. Carbon addition to the mixtures, caused increased porosity and improved energy dissipation efficiency in case of SE sample. In case of ASC, carbon addition caused a slight decrease in deformation, which is caused by changes in durability of diffusion bridges. They have been carburized, and the increase in carbon content increases the strength properties of the material. Observed slight deformations show, that there will be greater possibilities of energy absorption by the tested materials. Application of powder metallurgy makes it possible to easily regulate Fe Foam parameters, depending on the composition of the input materials without need to change the production technology.

Comparison of results is difficult due to the lack of standardization of metal foam

structures energy dissipation measurement methods, considering open-cell, closed-cell or syntactic foams. Comparison of results obtained with static tests such as quasi-static compression tests is more effective [25,26,27]. The results of dynamic tests received by the author were generated for a relatively small energy impact below 140 J, what resulted from ram device construction. Different results can be expected using the drop hammer in Pellini test.

5 CONCLUSIONS

The method of preparing metallic foams by powder metallurgy was presented. The processes of producing metallic foams by powder metallurgy are much more energy-efficient than other methods of producing porous Fe-based materials. This technology allows the production of metallic foams with open pores. The structures are controllable to some extent. The porosity depends on the size and shape of applied substrates. The chemical compositions of the sintered materials were selected to ensure proper filling the mould with foam so that it did not collapse.

SEM and optical microscope analysis were used to characterize the metal foams. Both techniques allowed determining differences in the materials microstructures. The levels of porosity in the sintered materials varied. Alloying additions integrated in the SE composition and finer particles size could lead to higher porosity levels. As the explanation of this phenomenon is not easy, there is a need for further research on sintered porous materials.

Studies of energy dissipation allowed to observe changes in the energy absorption level depending on the used foam material as well as its porosity. Research has shown that metallic foam materials have high energy absorption capacity and such studies are underway.

There are methods using liquid phase in porous materials producing technology (e.g. Lotus type), but they are significantly more expensive to implement for materials of comparable porosity.

Open-cell Fe-based foams may also find application as light-weight structural materials, or dissipative and energy-absorbing materials, or filters, catalyst substrates and heat exchange surface areas.

6 ACKNOWLEDGMENTS

Special thanks to Dr. Hab. Eng. Marek Jaśkiewicz with his team at the Faculty of Mechatronics and Mechanical Engineering, Dept. of Automotive Vehicles and Transportation, Kielce Technical University, for granting access to their equipment and devices used for mechanical testing.

7 REFERENCES

[1] M.F. Ashby, Metall. Trans. 14 A, (1983), pp. 1755-1769.

[2] van de Witte 1, P.J. Dijkstra, J.W.A. van den Berg, J. Feijen; Phase separation processes in polymer solutions in relation to membrane formation, Journal of Membrane Science 117 (1996) 1-31

[3] Jian-Hua Cao, Bao-Ku, Zhu You-Yi Xu; "Structure and ionic conductivity of porous polymer electrolytes based on PVDF-HFP copolymer membranes", Journal of Membrane Science, Volume 281, Issues 1–2, 15 September 2006, Pages 446-453

[4] John Banhart, Light-Metal Foams—History of Innovation and Technological Challenges; Advanced Engineering Materials, March 2013, DOI: 10.1002/ adem.201200217

[5] R. Orinakova, A. Orinak, L. Markusova Buckova, M. Giretova, L. Medvecky, E. Labbanczova, M. Kupkova, M. Hrubovcakova, K. Koval (2013), Iron Based Degradable Foam Structures for Potential Orthopedic ApplicationsInt. J. Electrochem. Sci., 8, pp. 12451-12465

[6] A.H. Brothers, R. Scheunemann, J.D. DeFouw, D.C. Dunand (2005) Processing and structure of open-celled amorphous metal foams. Scripta Materialia 52, pp. 335-339

[7] Arwade, J. Hajjar, B. Schafer (2011), Steel foam material processing, properties and potential structural applications. Structural Materials and Mechanics

[8] I. Mutulu, E. Oktay (2011), Processing and Properties of Highly Porous 17-4 PH Stainless Steel. Powder Metallurgy and

Metal Ceramics, Vol.50, Nos 1-2, pp. 73-82 UDC 621.762:621.793.79

[9] C. S. Y. Jee, Z. X. Guo, J. R. G. Evans, N. Özgüven (2000), Preparation of high porosity metal foams. Metallurgical and Materials Transactions B, Volume 31, Issue 6, pp. 1345-1352

[10] N. Bekoz, E. Oktay (2013), Mechanical properties of low alloy steel foams: Dependency on porosity and pore size. Materials Science and Engineering A, pp. 82 -90.

[11] T. Murakami, K. Ohara, T. Narushima, C. Ouchi (2007), Development of a New Method for Manufacturing Iron Foam Using Gasses Generated by Reduction of Iron Oxide. Materials Transactions, Vol. 48, No. 11 pp. 2937 - 2944.

[12] C. Park, S.R. Nutt (2001), Effects of process parameters on steel foam synthesis. Materials Science and Engineering A297, pp. 62-68.

[13] R. Chatys, W. Depczyński, W. Żórawski,: „Sposób wytwarzania struktur porowatych", Patent RP nr 199720

[14] W. Depczyński (2014), Sintering of copper layers with a controlled porous structure. METAL 2014 23rd International Conference on Metallurgy and Materials, pp. 1219-1224 WOS:000350641700201

[15] Wójcik T.M. (2012) Heat transfer enhancement and surface thermo stabilization for pool boiling on porous structures, EPJ Web of Conferences 25 01100

[16] T. Kujime, S. Hyun, H. Nakajima, (2006) Fabrication of Lotus – Type Porous Carbon Steel by the Continuous Zone Melting and Its Mechanical Properties. Metallurgical and Materials Transactions A Vol. 37A, pp. 393 - 398.

[17] M. Saadatfar, F. Garcia-Moreno, S. Hutzler, A.P. Sheppard, M.A. Knackstedt, J. Banhart, D. Weaire, (2009) Imaging of metallic foams using X-ray micro-CT. Colloids and Surfaces A, Physicochemical and Engineering Aspects 344, pp.107-012.

[18] W. Depczynski, Investigating porosity of sintering porous copper structure with 3D micro-focus X-ray computed tomography (uCT), (2014) Journal of Achievements in Materials and Manufacturing Engineering Vol.66, pp. 67-72.

[19] E. Maire et. al., (2014) Structural characterrization of solid foams, C. R. Physique

[20] W. Depczyński, R. Kazała, K. Ludwinek, K. Jedynak, (2016) Modelling and Microstructural Characterization of Sintered Metallic Porous Materials MATERIALS, Vol. 9, 567

[21] A. Rabei, L. Vendra, N. Reese, N. Young, B. P. Neville, (2006) Processing and Characterization of a New Composite Metal Foam. Materials Transactions, Vol. 47, No. 9, pp. 2148 - 2153.

[22] J. Marx, M. Portanova, A. Rabiei, (2018) A study on blast and fragment resistance of composite metal foams through experimental and modeling approaches, Composite Structures 194, pp. 652–661

[23] M. Garcia-Avila, M. Portanova, A. Rabiej (2014), Ballistic performance of a composite metal foam-ceramic armor system, Procedia Materials Science 4, pp. 151-156.

[24] [27] M. Garcia-Avila, M. Portanova, A. Rabiej, (2015) Ballistic performance of a composite metal foam, Composite Structures 125, pp. 202–211

[25] W. Depczynski, T. Miłek, Ł. Nowakowski (2017), Experimental comparison between upsetting characteristics of porous components prepared by Fe-based sintering technology, IOP Conference Series-Materials Science and Engineering 179 012015

[26] A. Rabiei, M. Garcia-Avila (2013) Effect of Various parameters on properties of composite steel foams under variety of loading rates, Materials Science & Engineering A 564, pp. 539-547

[27] Y.Alvandi-Tabrizi, D.A.Whisler, H.Kim, A.Rabiei, (2015) High strain rate behavior of composite metal foams, Materials Science&Engineering A631, pp. 248–257.